

Signal amplitude effects on reflectometer studies of density turbulence in tokamaks

T L Rhodes, W A Peebles, E J Doyle, P Pribyl, M Gilmore, R A Moyer†
and R D Lehmer†

Electrical Engineering and MANE Departments and Institute of Plasma and Fusion Research,
University of California, Los Angeles, CA 90095, USA

Received 23 June 1997, in final form 17 December 1997

Abstract. The effect of amplitude fluctuations on reflectometer measurements of density turbulence has been investigated through comparison of reflectometry and Langmuir probes on the CCT and DIII-D tokamaks. Power spectra, turbulent radial correlation lengths, and root-mean square magnitude variations (at the H-mode transition) of the homodyne reflectometer signal (given by $S_{Re} = E \cos(\phi)$, which depends strongly on the amplitude E and nonlinearly on the phase ϕ), show good agreement with Langmuir probes. The homodyne signal is found to be dominated by the amplitude fluctuations and not by the phase for high density fluctuation levels. Correspondingly, power spectra and correlation lengths deduced from the phase data alone show agreement with the homodyne signal only at low density fluctuation levels. It is concluded that for these plasma parameters the homodyne signal (S_{Re}) is closely representative of the density fluctuation behaviour and that this response is related to the reflectometer amplitude E . This correspondence of the homodyne signal and density fluctuations is in contrast to most theoretical/modelling work which has typically concentrated on the phase. A one-dimensional simulation of resonance absorption effects upon the amplitude and phase of a reflectometer is presented as an example of how amplitude fluctuations might arise due to processes internal to the plasma. The implications of these results and the connection to theory are discussed.

1. Introduction

Reflectometry has been used on many different plasma devices to monitor electron density fluctuations ([1–7] to name but a few early works). For example, qualitative changes in fluctuation level and Doppler shifts have been used to monitor the L- to H-mode transition [7], magnetohydrodynamic (MHD) behaviour [6, 7], as well as the radial correlation length of the density fluctuations [1]. Density fluctuations are thought responsible for turbulent transport of heat and particles in tokamak plasmas [8] making their measurement and characterization very important. Reflectometry has the distinct advantage of providing a local, non-perturbing measure of density fluctuations from the edge to the core of many high-temperature plasmas. A variety of reflectometry observations in plasmas appear inconsistent with models based on phase modulation brought about by Bragg scattering [9–13]. In this paper the role of fluctuations in the reflectometer signal amplitude (as well as the phase) is investigated as a possible explanation of these discrepancies. A comparison of the homodyne reflectometer signal (given by $S_{Re} = E \cos(\phi)$ which depends strongly on the amplitude E and nonlinearly on the phase ϕ) and Langmuir probe data shows broad agreement in power

† Fusion Energy Research Program, University of California, San Diego, CA 92093, USA.

spectra and correlation lengths. At high density fluctuation levels the evidence indicates that the homodyne signal is dominated by the amplitude fluctuation and not by the phase. The results are compared with recent models to illustrate consistency and areas of disagreement. Finally, the effect that a localized absorption or loss (e.g. resonance absorption) would have on a reflectometer signal is numerically investigated as an example of how amplitude fluctuations might arise due to internal plasma processes (other models include the effect of amplitude fluctuations but these are principally due to interference-type effects).

1.1. Brief overview of reflectometry for density fluctuation diagnosis

Reflectometry consists of launching electromagnetic radiation (generally millimetre-wave or microwave frequencies for fusion research plasmas) towards the plasma to be investigated. The radiation propagates in the plasma until it reaches a cut-off density defined by the local electron density and magnetic field [14]. For O-mode propagation (i.e. where the electric field E_{rf} of the reflectometer beam is parallel to the local magnetic field B) the signal reflects (or is cut off) at the position where the reflectometer frequency f_{rf} equals the local plasma frequency $f_{pe} = (n_e e^2 / (2\pi)^2 \epsilon_0 m_e)^{1/2}$. Here n_e is the local electron density, e is the electron charge, ϵ_0 is the vacuum permittivity, and m_e is the electron mass. For X-mode propagation ($E_{rf} \perp B$) cut off occurs where f_{rf} equals either

$$f_{rh} = f_{ce}/2 + [(f_{ce}/2)^2 + f_{pe}^2]^{1/2} \quad \text{or} \quad f_{lh} = -f_{ce}/2 + [(f_{ce}/2)^2 + f_{pe}^2]^{1/2}.$$

Here f_{rh} and f_{lh} refer to the right- and left-hand cut-off frequencies and $f_{ce} = eB/(2\pi m_e)$ is the local electron cyclotron frequency. The beam is reflected from this cut-off region and it is this reflected radiation that is detected and recorded. During propagation and reflection the beam is subject to both refraction and diffraction (including scattering processes) and absorption effects [14, 15]. If there are no density fluctuations the returned signal is constant in time, whereas if the density varies (and/or if the magnetic field varies for X-mode propagation) the reflectometer signal will also change. For small enough density fluctuation levels it has been theoretically shown that the phase fluctuations of the reflectometer signal are proportional to the electron density fluctuations, $\phi(t) = \alpha n_e(t)$ [4, 15–19]. It is for this reason that the majority of theoretical and experimental work has concentrated on the phase response of the reflectometer signal. Note that the parameter α is generally a function of fluctuation and reflectometer wavelengths, and index of refraction scale length [17, 19], and can also depend on the shape of the density perturbation [19].

One- and two-dimensional modelling predict that density perturbations along the path can scatter the incident reflectometer wave towards a receiver if certain restrictions on the perturbation wavenumber are met [4, 16–18, 20]. These restrictions arise from momentum and energy conservation of the interacting waves and are quantified in a wavenumber selection or matching condition given by $k_{\tilde{n}} = 2k_{rf} \sin(\theta_s/2)$. This relation is commonly referred to as the Bragg scattering rule due to its similarity with acousto-optics and conventional plasma scattering. Here $k_{\tilde{n}}$ is the wavenumber of the plasma perturbation and k_{rf} is the reflectometer wavenumber in the plasma, $k_{rf} = k_0 N(r)$, $N(r)$ is the local plasma index of refraction at position r , k_0 is the vacuum reflectometer wavenumber, and θ_s is the scattering angle between the perturbation and probe wavenumbers. For pure backscattering, that is scattering directly back towards the launch antenna, $\theta_s = \pi$ so that $k_{\tilde{n}} = 2k_{rf} = 2k_0 N(r)$. Backscattering can also occur for the wave reflected from the cut-off which is backscattered back towards the cut-off where it undergoes a second reflection and is then received by the reflectometer. Forward scattering can occur when θ_s is a small angle and either (a) the reflected signal is scattered directly into the receive antenna or

(b) the incident radiation is first scattered and then is reflected from the cut-off layer back into the receiver. Since $N(r) \leq 1$ in a plasma, the Bragg scattering rule indicates that only wavenumbers $k_{\tilde{n}} \leq 2k_0$ can cause scattering (either directly or indirectly) into the receiver, that is for $k_{\tilde{n}} > 2k_0$ no signal should be observed by the reflectometer [4, 16, 17]. Also, since $N(r)$ is in general a function of position, different plasma perturbations $k_{\tilde{n}}$ will scatter from different regions of the plasma thus producing a response which is not localized to the cut-off layer. However, experimental work in a laboratory plasma found that the reflectometer signal was dominated by perturbations near the cut-off layer and that this position did not change with perturbation wavenumber [9, 11]. Both an amplitude and phase modulation were observed as well as a response well above the value $k_{\tilde{n}} = 2k_0$. In that work [11] the observations were found to be inconsistent with the one-dimensional (1D), full-wave modelling performed therein and it was conjectured that the difference was due to three-dimensional (3D) effects neglected in 1D models.

1.2. Structure of reflectometer signal

The reflectometer signal $S(t)$ is, in general, complex and composed of both a phase $\phi(t)$ and amplitude $E(t)$ component,

$$S(t) = E_{\text{LO}} E(t) e^{i\phi(t)}. \quad (1)$$

Here it is assumed that the signal is combined in a mixer with a local oscillator (LO) signal of the same frequency as the original reflectometer probe beam, where E_{LO} is the LO electric field, and $\phi(t)$ is the reflectometer signal phase relative to the LO phase. The reflectometer signal as it would appear on the output of a mixer in the laboratory is given by the real part of equation (1):

$$S_{\text{Re}}(t) = \text{Re}[S(t)] = \text{Re}[E_{\text{LO}} E(t) e^{i\phi(t)}] \quad (2)$$

(where Re designates the real part of the expression). Equation (2) is often referred to as the homodyne reflectometer signal. Note that the homodyne signal includes both amplitude $E(t)$ and phase $\phi(t)$ components. Quadrature detection techniques can be used to obtain the imaginary part (S_{Im}) of equation (1) as well. Using $E(t) = E_0 + \tilde{E}$ and $\phi(t) = \phi_0 + \tilde{\phi}$, equation (1) becomes

$$S(t) = (E_0 + \tilde{E}) e^{i\tilde{\phi}} = E_0 e^{i\tilde{\phi}} + \tilde{E} e^{i\tilde{\phi}}. \quad (3)$$

Here \tilde{E} and $\tilde{\phi}$ are the time varying parts of E and ϕ , respectively, and the time averages are given by $\langle E(t) \rangle = E_0$ and $\langle \phi(t) \rangle = \phi_0$. In equation (3) E_{LO} and $e^{i\phi_0}$ have been suppressed for clarity. The time-dependent amplitude component $\tilde{E}(t)$ may vary due to absorption, refraction and/or diffraction (including scattering), or interference effects or a combination of all of these. The phase $\tilde{\phi}(t)$ can vary due to changes in $\tilde{E}(t)$ (due, for example, to a temporally varying signal size [21]) or electron density either along the beam propagation path or at the cut-off layer or a combination thereof. For $\tilde{\phi}$ small, equation (3) becomes approximately linear in $\tilde{\phi}$:

$$S(t) \simeq E_0 \left(1 + \frac{\tilde{E}}{E_0} + i\tilde{\phi} \right) \quad (4)$$

where second-order and greater terms have been neglected. The homodyne signal S_{Re} is then the real part of equations (3) or (4). It is observed that the reflectometer signal S is linear in \tilde{E} for all values of \tilde{E} (equations (3) and (4)) while it is linear in $\tilde{\phi}$ only for $\tilde{\phi}$ small, i.e. equation (4). Theory has shown that the phase fluctuation is proportional to the density fluctuation level, $\tilde{\phi} \propto \tilde{n}_e$, for small enough \tilde{n}_e . Most of the early reflectometer models

assumed equation (4) and further that $\tilde{E} = 0$. This has led to the experimental emphasis on the phase of the reflectometer signal. In this paper, evidence for the importance of \tilde{E} (in both high and low fluctuation regimes, equations (3) and (4), respectively) and its close connection to density fluctuations is presented.

The paper is organized as follows: section 2 describes the experiments and presents results of comparisons between reflectometer and Langmuir probe measurements. Section 3 is a comparison of the reflectometer data to some current reflectometer models. This section also includes results from 1D numerical modelling of the effect of resonance absorption upon the reflectometer signal. Section 4 is a summary and conclusion.

2. Comparison of reflectometer and Langmuir probe fluctuation data

A comparison of reflectometer and Langmuir probes was performed on both the CCT and DIII-D tokamaks. A description of the CCT tokamak is presented first with the description of the DIII-D experiment given later. The CCT tokamak is a circular cross section, ohmically heated tokamak with major radius $R_0 = 1.5$ m, minor radius $a = 40$ cm, plasma current $I_p = 10$ kA, toroidal magnetic field $B_z = 0.2$ T, pulse length $t_p = 200$ ms, and central densities and electron temperatures of $n_e \simeq 3 \times 10^{12}$ cm $^{-3}$ and $T_e \simeq 100$ eV.

The reflectometer system used for the CCT comparison was located on the outboard midplane. It was operated using O-mode polarization with a frequency range of 8–12 GHz. This frequency range corresponds to a vacuum wavelength of 3.75–2.5 cm and a cut-off density range of 0.8 – 1.8×10^{12} cm $^{-3}$. The Langmuir probe array was also located on the outboard midplane toroidally displaced from the reflectometer by approximately 5 degrees. The probes were biased so as to collect ion saturation current $I_{\text{sat}} = An_e T_e^{1/2}$, where n_e and T_e are the local electron density and temperature, respectively, and A is a constant which depends upon the probe size and geometry, ion mass and charge, etc (a pure hydrogen plasma is assumed such that $n_i = n_e$). For small electron temperature fluctuations it can be shown that the fluctuation in the ion saturation current is approximately proportional to the density fluctuation, $\tilde{I}_{\text{sat}}/I_{\text{sat},0} \simeq \tilde{n}/n_0$. A more detailed description of the reflectometer and probe systems can be found in [12].

Langmuir probes provide a localized measurement of \tilde{n}_e and are sensitive to many wavenumbers, radial, poloidal, and toroidal (k_r , k_θ , k_z). As discussed in the introduction, reflectometer modelling and theory generally predict that the reflectometer responds to density fluctuations as dictated by the Bragg wavenumber selection formula, $k_{\tilde{n}} = 2k_{\text{rf}} \sin(\theta_s/2)$ (see [19] for the effect of the shape of the modulation on the modelled reflectometer response). However, these predictions refer solely to the reflectometer phase and not the amplitude.

In the following, the reflectometer–probe comparison data are presented first as power spectra, followed by time histories, and then turbulent radial correlation lengths. From these data it can be concluded that the homodyne signal is closely representative of the density fluctuations. Furthermore, at high fluctuation levels the homodyne signal is dominated by the amplitude and not by the phase. Measurements show that the phase agrees with the homodyne signal only at low fluctuation levels. These results are then discussed in relation to current modelling in section 3.

2.1. Comparison of power spectra

Figure 1 compares the power spectra from a Langmuir probe and a homodyne reflectometer signal S_{Re} (equation (2) or alternatively the real part of equation (3) or (4)) for an ohmic

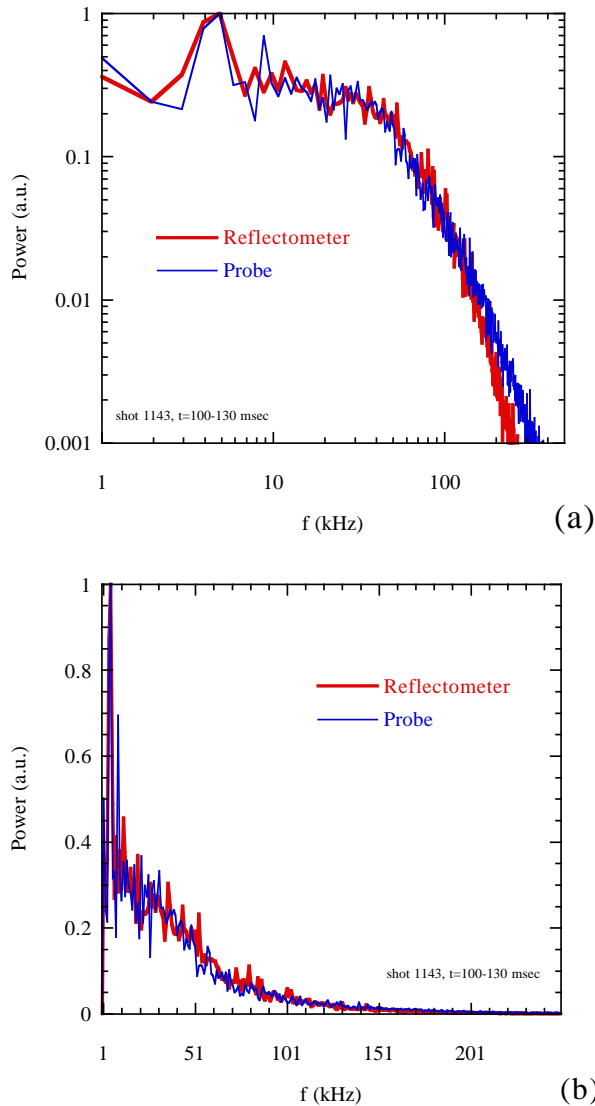


Figure 1. Comparison of power spectra from homodyne reflectometry and Langmuir probes in an ohmic (high level density fluctuation regime) CCT discharge plotted using: (a) log–log scale and (b) linear scale.

discharge on CCT. The detection positions of the reflectometer and probe are $r/a \simeq 0.8$ and the data are averaged over 30 ms during the flat top portion of the discharge. The same data are shown using both logarithmic and linear scales in order to see the close correspondence at all but the highest frequencies. The relatively narrow MHD-type mode at ~ 5 kHz and the broadband activity up to ~ 200 kHz are observed by both diagnostics. Furthermore, it is not just the general characteristics but also the detailed spectral shape that is in agreement between the two. This type of agreement in spectral shape has been reported on other machines ([3] for homodyne spectra and [5] for phase spectra) although it has never been discussed in detail. The time chosen for this comparison was a time when the two signals

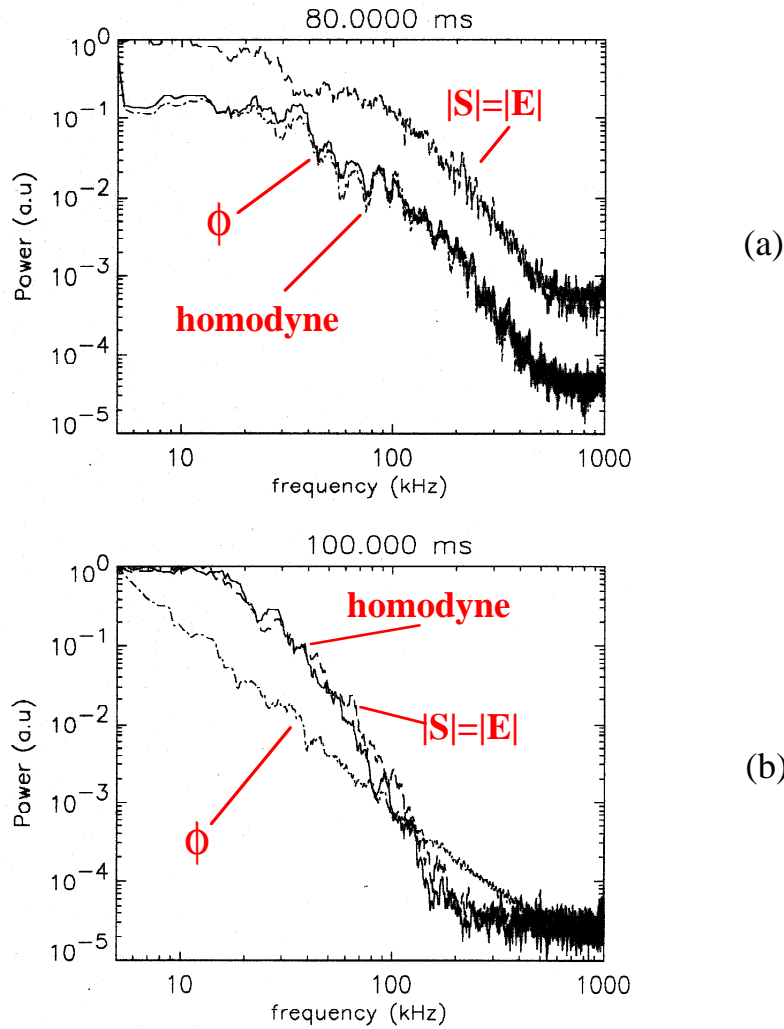


Figure 2. Homodyne, phase and magnitude power spectra from CCT reflectometry for (a) low density fluctuation level regime (H-mode), note that $|S|$ is offset for clarity, and (b) high density fluctuation level regime (ohmic).

had a relatively high cross correlation indicating that the two diagnostics were observing the same density structures. Similar good agreement was observed on other plasma discharges.

Reflectometer data were also obtained on CCT using a quadrature system. The system is similar to that detailed in [12] with the two balanced mixers replaced with quadrature mixers. Such a system can separate the phase and amplitude contributions to the complex reflectometer signal $S(t)$ (equation (1)). Figure 2 shows the resulting power spectra obtained from the homodyne ($E \cos(\phi)$), phase (ϕ), and magnitude ($|S|$) components of the reflectometer signal. Two CCT conditions are shown: a biased H-mode [22] and an ohmic discharge (figures 2(a) and 2(b), respectively). Ohmic CCT discharges have large edge fluctuation levels, typically $n_{e,\text{rms}}/n_{e,0} = 20\text{--}60\%$ at the edge which can decrease by as much as a factor of two in H-mode (e.g. figure 4, next section). Figure 2(a) (H-mode

data) shows that there is very close agreement between the homodyne and phase spectra for low-density fluctuation levels and agreement in shape between the phase/homodyne data and the magnitude data $|S|$. In figure 2(a) the magnitude spectrum $|S|$ is artificially offset to clearly show the agreement between the phase and homodyne data as well as the small scale differences in the magnitude data. The magnitude spectrum ($|S|$) differs in detail, but not in general shape, from the homodyne spectrum in both fluctuation level cases. This can be explained by noting that the magnitude $A(t) = |S(t)|$ is always positive, whereas the homodyne signal S_{Re} can be either positive or negative. In contrast, the ohmic data (i.e. high fluctuation levels, figure 2(b)) show a distinct difference between the homodyne and phase spectra. The phase spectrum falls off as $1/f^2$ (in agreement with the theory of [23] to be discussed later) and is thus very different from any power spectra measured by Langmuir probes. These spectra also indicate that the homodyne signal is dominated by the amplitude fluctuation in the high-density fluctuation level case (figure 2(b)).

Figure 3 shows a comparison of homodyne reflectometry and Langmuir probe data from the DIII-D tokamak [24] for a quite different set of plasma parameters. The DIII-D tokamak is a large fusion research tokamak of major radius ~ 1.67 m, minor radius ~ 0.67 m, $I_p \simeq 2$ MA, $B_z \simeq 2.1$ T, elongation ~ 1.8 , central electron densities and temperatures of approximately $6 \times 10^{13} \text{ cm}^{-3}$ and 2 keV, respectively. Both the reflectometer and probe

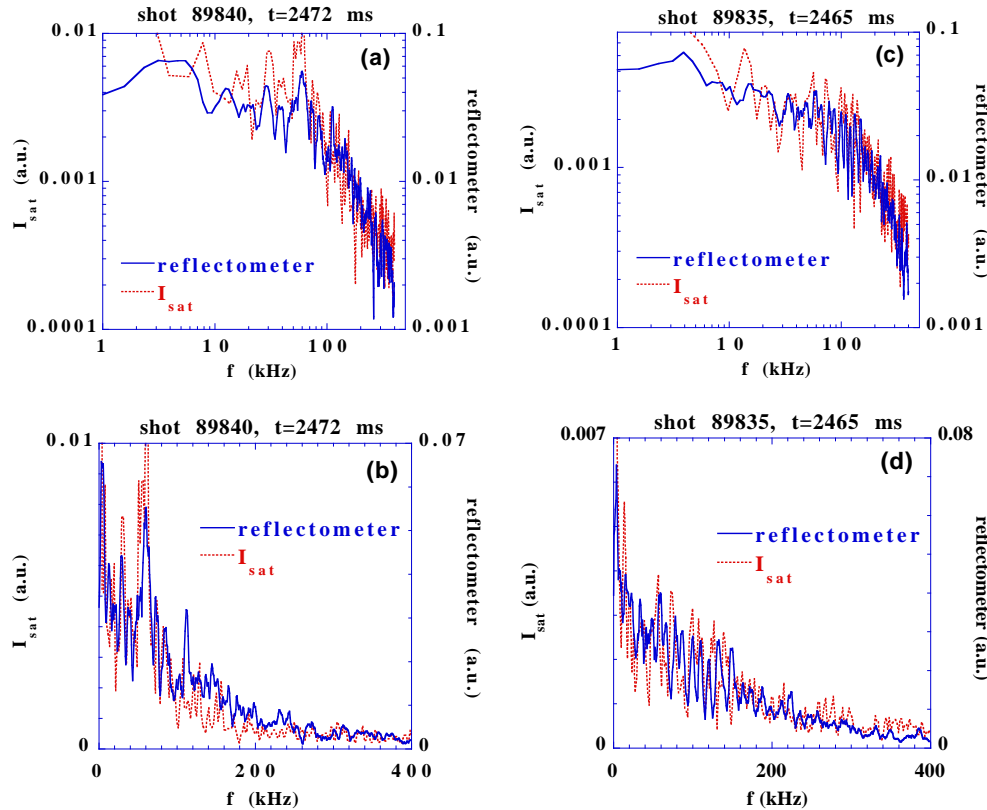


Figure 3. Comparison of power spectra from homodyne reflectometry and Langmuir probes on DIII-D showing: (a) linear scale; and (b) log scale of coherent mode activity in H-mode; (c) linear scale; and (d) log scale of broadband fluctuations during L-mode.

systems were located at nearly the same toroidal position but separated by approximately 17 cm in the poloidal direction. The cross correlation between the two diagnostics was thus very low. This is very different from the CCT data where the reflectometer and probe were separated in the toroidal direction where the toroidal correlation length is long compared to the poloidal. Figure 3 shows two different discharges, one with coherent mode activity (at 60 kHz, figure 3(a)) and one without (figure 3(b)). The reflectometer (homodyne) was operated in O-mode at 32 GHz (0.94 cm vacuum wavelength) and was reflecting from a radial position very near that of the probe (as determined from equilibrium fitting codes, Thomson scattering profiles, and the measured probe position). The data from the two diagnostics are similar in both general spectral shape and in the large coherent mode activity. For a probe position closer to the tokamak wall, agreement in spectral shape was found between the probe and the 24 GHz O-mode reflectometer, whereas the 32 GHz signal was dissimilar at that time as compared to the probe.

2.2. Comparison of fluctuation level time history

A comparison of time history of the magnitude of the fluctuations as measured by Langmuir probes and reflectometry on CCT is shown in figure 4. A biasable electric probe was inserted into CCT which sets up a radial electric field and a net radial current. If large enough, the sheared electric field can reduce the fluctuation level and induce a biased H-mode [22]. For the case presented here, the bias was varied sinusoidally creating an oscillating reduction in fluctuation level. Figure 4 shows a time history of the root-mean-square (RMS) saturation current $I_{\text{sat,rms}}/I_{\text{sat,0}} \simeq n_{\text{e,rms}}/n_{\text{e,0}}$ and the RMS homodyne reflectometer signal S_{rms} . Both signals are summed over the same frequency range 1–500 kHz and are thus a measure of the total fluctuating amplitude at that time. The probe signal shows a periodic reduction in fluctuation level (i.e. at 84, 101, and 119 ms) as the bias current is varied. The RMS reflectometer signal S_{rms} shows a close correspondence in both time and magnitude variation with the probe. The fluctuation reduction at the H-mode transition is of the order of 30% and is consistent with the reductions observed on other shots which produced H-mode plasmas

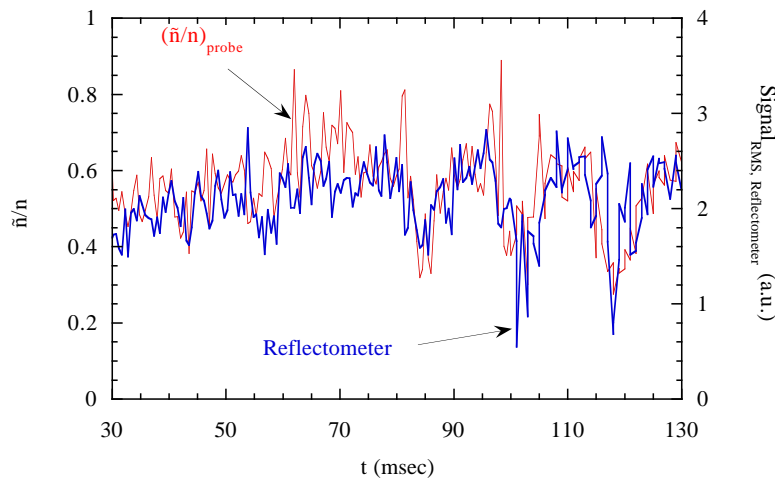


Figure 4. Time history of RMS levels from homodyne reflectometry and Langmuir probes on CCT showing low and high level density fluctuation regimes.

[25]. It is quite remarkable that the reflectometer shows such agreement over the large range of $n_{e,\text{rms}}/n_{e,0}$ shown. These data are interpreted as indicating that the homodyne signal S_{Re} is closely related to $n_{e,\text{rms}}/n_{e,0}$. Note that the magnitude of S_{Re} depends upon target size and distance as well as antenna pattern, conversion loss, etc all of which should be taken into account for a radial determination of $n_{e,\text{rms}}$.

2.3. Comparison of radial correlation lengths

A comparison of turbulent radial correlation lengths from an ohmic discharge on CCT is shown in figure 5. A 10 pin linear Langmuir probe array was used to collect the probe data. Each pin was radially separated from its neighbour by 2 mm and biased into ion saturation to monitor density fluctuation behaviour. Data were obtained from a sequence of discharges building up the correlation function using different pair separations. The reflectometer data (O-mode) were collected similarly using different frequency separations for each shot and thus building up the correlation as a function of separation. More details on the system can be found in [12]. Here it is the homodyne signal S_{Re} (equation (2)) which is used. The density profile was not measured in detail for these discharges but was instead inferred from a single interferometer chord constrained by edge Langmuir probe profiles. The resulting set of density profiles was then used to convert the reflectometer probing frequency to spatial location. This resulted in the dominant uncertainty in the reflectometer correlation length (typically $\pm 50\%$). From figure 5 one finds that the probe correlation length varies from ~ 2.5 cm at 20 kHz to ~ 0.5 cm at 150 kHz. This is within the normal range of lengths reported from other tokamaks [26–29]. The reflectometer data show a similar trend of decreasing correlation length with increasing frequency. Importantly, there is quantitative agreement within the error bars indicating that the homodyne correlation length is a good representation of the density fluctuation behaviour.

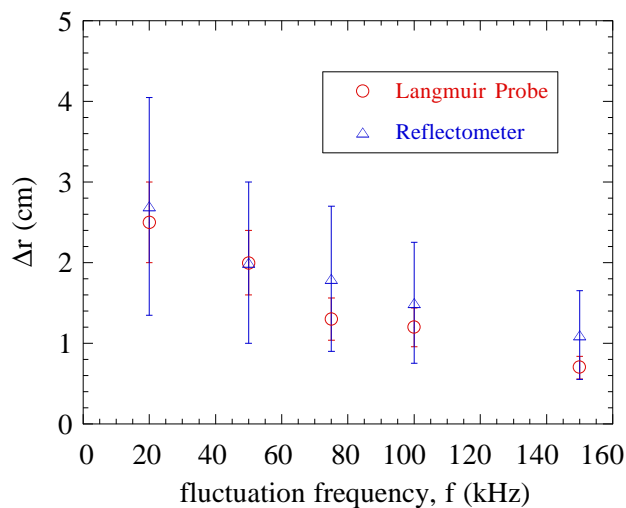


Figure 5. Comparison of radial correlation lengths from homodyne reflectometry and Langmuir probes from ohmic CCT conditions.

Correlation length data were also obtained using a quadrature correlation reflectometer system [12] on CCT. It was found that the correlation length obtained from the phase fluctuation is always less than that from the homodyne for ohmic conditions (i.e. at high

fluctuation levels). As the fluctuation level decreases the phase correlation length approaches that of the homodyne signal. From this one concludes that the close correspondence of correlation lengths between the reflectometer and probe (figure 5) is due to the amplitude portion of the homodyne reflectometer signal rather than the phase. At low fluctuation levels the amplitude and phase response are similar indicating that either could be used.

2.4. Discussion of experimental results

From the data presented above it appears that the homodyne signal S_{Re} can be closely representative of the density fluctuation behaviour (power spectra, correlation length, etc). Good agreement with Langmuir probes was found over a significant range in density, magnetic field, and reflectometer wavelength on two very different tokamaks. For low fluctuation levels (e.g. H-mode) the phase follows the homodyne signal but this behaviour is lost as the fluctuation level increases. At higher fluctuation levels an unphysical (in terms of the density fluctuations) $1/f^2$ spectrum is observed in the phase spectra. Thus it appears that at high fluctuation levels the homodyne signal is a good representation of the density fluctuation behaviour while at low fluctuation levels either the homodyne or phase signal can be used. The data are interpreted as indicating that it is the amplitude part of the reflectometer signal that most closely represents the \tilde{n}_e behaviour at the higher fluctuation levels. Equation (3) shows that the reflectometer signal is linear in \tilde{E} for all values of \tilde{E} but is linear in $\tilde{\phi}$ only for $\tilde{\phi}$ small, i.e. equation (4). This is believed to be an indication as to why the homodyne signal appears more closely aligned to the density fluctuations, at high fluctuation levels, than is the phase. The source of the amplitude fluctuation \tilde{E} remains to be identified but could be due to the effect of absorption, target area changes due to a rippled mirror type effect, or other mechanisms. This is discussed in more detail in the next section. There is some indication that the homodyne signal ($S_{\text{Re}} = E \cos(\phi)$) is a closer representation of the density fluctuation behaviour than is the magnitude ($|S| = E$) alone. The reason for this is not well understood at this time. An example of this can be found in the good agreement between the phase and homodyne spectra in contrast with the small differences seen between the phase and the magnitude spectra (figure 2(a)). The correlation was also better between the phase and homodyne signal than between the phase and the magnitude for this low fluctuation regime data. These differences could be due to the fact that the magnitude $|S|$ is a nonlinear function of the real and imaginary parts of the reflectometer signal, $|S| = (S_{\text{Re}}^2 + S_{\text{Im}}^2)^{1/2}$. In addition, the homodyne signal carries some information about the sign of the fluctuation, that is, the homodyne signal can be either positive or negative, unlike the magnitude which is always positive.

The wavenumber response expected from the CCT reflectometer (based on the 1D Bragg selection rules) is $k_{\text{max},10 \text{ GHz}} \leq 4 \text{ cm}^{-1}$ and for the DIII-D reflectometer $k_{\text{max},32 \text{ GHz}} \leq 13 \text{ cm}^{-1}$. The maximum wavenumber response of the probes is set by their physical dimensions and is approximately 30 cm^{-1} and 21 cm^{-1} for CCT and DIII-D, respectively. Thus the wavenumber sensitivities of both diagnostics encompass the expected turbulent wavenumber range ($0\text{--}2 \text{ cm}^{-1}$ [26–29]) in CCT and DIII-D. Using the Bragg scattering picture, the fluctuation signal should come from very near the cut-off layer on DIII-D indicating good expected spatial resolution and in agreement with the comparison to probe data. However, on CCT the fluctuations are predicted to come from a $\sim 2.5 \text{ cm}$ layer extending from the cut-off towards the vacuum region. Given the good correlation between the CCT reflectometer and probes, and the fact that this high correlation occurs only at certain times, indicates that the CCT data are better localized than these models would predict.

Some discussion of the magnitude of the correlation lengths as measured by the reflectometer is in order here. The measured CCT reflectometer correlation lengths (1–3 cm) are shorter than the vacuum wavelength (in this case $\lambda_0 \sim 3$ cm) by a factor of 33–100%. Full-wave, 1D simulations indicate that the lengths measured using the reflectometer phase should not be less than approximately four to eight times the vacuum wavelength [17]. This is somewhat modified in 2D where Bruskin *et al* [30] conclude from a 2D full-wave simulation that phase correlation lengths of the order of the vacuum wavelength are possible. The 2D model of Mazzucato and Nazikian [23] indicates that the phase correlation length can be less than the vacuum wavelength (for high fluctuation levels) but that this is not the correlation length of the turbulence. In that model, at low fluctuation levels, the phase correlation length does recover the correct turbulent correlation length while at higher fluctuation levels a correlation length correction factor can sometimes be applied. These and other similar phase calculations are the basis of the conclusion that a reflectometer can never measure a real correlation length less than the vacuum wavelength[†]. The fact that these simulations work with the radial correlation of the phase and not the homodyne signal is proposed as an explanation of the difference between these theories and the data presented here.

As noted, modelling [17, 23] indicates that a correction term to the phase correlation length can sometimes be applied. This should strictly be applied only to the phase measurement; however, it is of interest to ask how such a correction would affect the homodyne reflectometer data of figure 5. A correction factor of $\sim 1/4$ for the 1D case [17] and ~ 3 for the 2D case (in the model of [23] the correction needed for a high fluctuation level is just the RMS phase fluctuation which for these conditions is ~ 3 radians) would move the reflectometer values well outside the Langmuir probe error bars. One concludes that the correlation lengths obtained from the homodyne signal have a significantly different behaviour than those from the phase.

Measurements of homodyne radial correlation lengths in the steep H-mode edge of DIII-D find quite short lengths compared to the vacuum wavelength, for example a ratio of (figure 6)

$$\frac{\text{correlation length}}{\text{vacuum wavelength}} \simeq \frac{0.2 \text{ cm}}{0.5 \text{ cm}}.$$

In this steep density gradient region, where the density scale lengths are ~ 1 cm, a correlation length which was a significant fraction of the density scale length would be unphysical, as then two density layers, differing in density by a factor of two to three, would be well connected in terms of fluctuations. Density fluctuation driven transport would then cause a collapse of the steep profiles which is not observed. Furthermore, Langmuir probe measurements in the transport barrier region indicate a strong variation in the magnitude of the fluctuations within a ~ 0.5 cm region [32] in contradiction to a long radial correlation length (i.e. >0.5 cm). Thus, although the measured correlation lengths can be short

[†] As an interesting sidenote, the conclusion that a reflectometer cannot measure a real turbulent correlation length less than the vacuum wavelength arises from the simulations on the phase and is not necessarily a physical limit. For example, in the last 10 to 15 years there has been considerable work in the area of near-field microscopy wherein resolutions better than $1/30$ of the probe wavelength have been reported (for an example using microwaves see [31]). This method relies on modification of evanescent waves within a small aperture which results in propagation of a portion of this originally evanescent field. The aperture dimensions are less than the probe wavelength and it is these dimensions which determine the spatial resolution. The method generally uses the intensity of the received radiation although the phase is sometimes used. It may be of interest to investigate the applicability of this effect to reflectometry. In that case, aperture effects could arise due to overdense plasma clumps or ridges perpendicular to the incident probe beam which have a small underdense central region through which the radiation could pass.

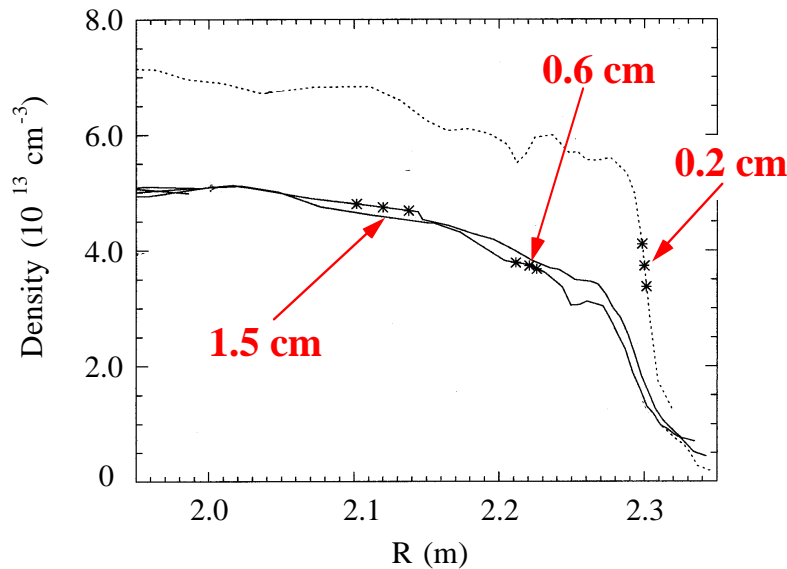


Figure 6. Correlation lengths from homodyne reflectometry are indicated where they occur on DIII-D density profiles for L-mode and H-mode plasmas. Short correlation lengths are found in the transport barrier region of H-mode plasmas.

compared to the vacuum reflectometer wavelength, the comparison to probes (CCT) and to density scale lengths and fluctuation structure (DIII-D) indicate that these values are physical from the perspective of plasma fluctuations.

3. Comparison to reflectometry models

The homodyne signal S_{Re} is, in general, closely representative of the density fluctuations in the data shown above (both CCT and DIII-D) with the evidence indicating that this agreement is due to the amplitude portion of S_{Re} . However, it is not yet clear from a theoretical perspective how this might be so. Most theoretical work has dealt with the reflectometer phase response to a fluctuating density field ignoring the amplitude response or assuming it constant. For example, [4, 16, 17] address the phase response to a density perturbation without an amplitude variation in the reflectometer signal ([16] does consider a spatially, but not temporally, varying amplitude due, for example, to refraction or absorption). More recently, several models have emerged which do include the amplitude fluctuations [18, 23, 33]. In the following, the models of [23, 33] are discussed in light of the data presented above. Agreement is found on several points for both models with some areas of disagreement. After this discussion a numerical 1D, full-wave model of resonance absorption effects upon a reflectometer signal is presented. This model is presented as an example (rather than an explanation) of how intrinsic reflectometer amplitude variations might arise within a plasma and what their effect would be upon the signal.

3.1. Comparison with random phase screen model [23]

The model of reference [23] predicts that at low fluctuation levels (defined with respect to the probe wavelength and local permittivity scale length) the reflectometer phase and

amplitude, as observed outside the plasma, are closely related to the density perturbation. In this model, $\tilde{\phi}$ at the cut-off layer is assumed to be due to a phase grating which arises from plasma density fluctuations so that $\tilde{\phi} \sim \tilde{n}_e$. The structure of the random phase grating can have many different wavenumbers which then produce $\tilde{\phi}$ with corresponding wavenumbers. The model then propagates these different wavenumber perturbations back to the receiver plane where the possibility of interference arises. This interference gives rise to phase as well as amplitude fluctuations in the received reflectometer signal. At low fluctuation levels the interference effects are negligible and the density fluctuation behaviour can be extracted from the phase fluctuations. At these low fluctuation levels the reflectometer signal at the cut-off layer is approximated by $S \simeq E_0 e^{i\tilde{\phi}} \simeq E_0(1 + i\tilde{\phi})$, i.e. equation (4) with $\tilde{\phi} \ll 1$ and $\tilde{E} = 0$, so that the phase is then given by $\tilde{\phi} \simeq \text{Im}[S/E_0]$. Note that there is no intrinsic amplitude fluctuation at the cut-off layer, i.e. the second term on the right-hand side of equation (3) is zero at the cut-off layer (although there can be large amplitude fluctuations at the receiver). This small fluctuation level case is similar to the data shown in figure 2(a) above where the fluctuations are small and the power spectra of the homodyne and phase are almost identical. For high fluctuation levels the model predicts a phase power spectra decay of $P_\phi(f) \sim f^{-2}$ in agreement with the data in figure 2(b) both in terms of shape and also the fluctuation level regime.

The phase data shown in this paper are thus consistent with the Mazzucato and Nazikian model for both high and low fluctuation regimes. At higher fluctuation levels the model predicts that neither the phase nor the amplitude fluctuations (as observed at the receiver) are representative of the density perturbation. This prediction does not appear to agree with the CCT homodyne data in figures 1, 4, and 5, where there is good agreement between the homodyne signal and probes yet the fluctuation level is high enough that the phase and amplitude spectra are dissimilar (figure 2(b)). One interpretation of these observations is the following. The fluctuating reflectometer signal S in [23] is due to the interference of phase components with different wavenumbers originating at the cut-off layer. A departure from that prediction (that is significant agreement between the homodyne signal and \tilde{n}_e) could be due to the domination of S by a mechanism other than this interference, for example an \tilde{E} due to amplitude variations/losses at or near the cut-off layer. The CCT/DIII-D data suggest a model in which S is dominated not by interference effects (although interference is surely present) but rather by intrinsic amplitude fluctuations arising from within the plasma.

3.2. Comparison with distorted mirror model [33]

A second model that includes 2D effects and amplitude variation is that of reference [33] where the plasma cut-off layer is modelled as a rough reflecting mirror surface that scatters the incident radiation. In this model, amplitude variations arise from a loss of signal due to scattering out of the receiver acceptance angle as well as interference effects. Since the cut-off layer is assumed to be a rippled mirror it follows that the spatial localization should be very good. An important and unresolved issue in this model is how to relate the reflectometer signal to the actual plasma density fluctuation levels.

For small surface roughness (up to $\sim 10\%$ in the paper), the model predicts an approximately linear increase in the incoherent scattering coefficient as the surface roughness is increased. Note that this is a prediction on the amplitude fluctuation level. This is quite similar to the data shown in figure 4 where the RMS reflectometer signal closely tracks the density fluctuation level as given by the Langmuir probe. The study also finds that poloidal correlation lengths inferred from the reflectometer measurement are consistent with Langmuir probe measurements. Since the plasma is modelled as a rough reflecting surface

the radial correlation lengths obtained by reflectometry should agree with the real density correlation lengths. This is to be compared with the agreement found herein between the reflectometer and the radial correlation lengths from probes.

The data presented in this paper are found to be in qualitative agreement with the model. The detailed application of the model to the present data involves measurements and parametrizations of the reflectometer system which are not now available. Thus a more quantitative comparison of this model to the data presented here cannot be made.

3.3. 1D, full-wave resonance absorption model

The data presented in section 2 indicate that amplitude variations are important in the reflectometer signal. From the comparison with the model of reference [23] it also appears that these amplitude fluctuations most probably arise from interactions within the plasma and not from interference effects at the detector. The question that arises is how might these variations arise and what is the effect on the reflectometer signal? As an example of a source of amplitude variation, a 1D, full-wave simulation of resonance absorption effects has been performed. The resonance absorption process [34–36] couples energy from an O-mode reflectometer probe beam to plasma oscillations and can cause a time-dependent variation of the reflectometer signal. Resonance absorption can occur whenever the electric field of the probe beam is aligned with the local density gradient (due to refraction, beam misalignment, etc). The probe electric field then drives density fluctuations at the reflectometer probe frequency f_{rf} . If this frequency is near the electron plasma frequency, f_{pe} resonance occurs and energy can be coupled from the electromagnetic field to the plasma oscillations. This effect can thus be important near the cut-off for O-mode propagation where $f_{\text{rf}} = f_{\text{pe}}$. The magnitude of the resonant density fluctuation is limited by collisional effects.

The resonance effect is modelled using a 1D, full-wave calculation of the reflectometer–plasma system similar to that in [17], except with the inclusion of resonance absorption effects. The relevant equation is modified according to [34, 36]

$$\frac{d^2 B(r)}{dr^2} - \frac{1}{\epsilon(r)} \frac{d\epsilon(r)}{dr} \frac{dB(r)}{dr} + k_0^2 [\epsilon(r) - \sin^2(\theta)] B(r) = 0$$

where $\epsilon(r)$ is the local index of refraction, θ is the angle of incidence of the reflectometer beam with respect to the density gradient, and B is the reflectometer magnetic field. The code calculates the reflectometer magnetic field using a finite-difference algorithm with initial conditions in the evanescent region, i.e. where the index of refraction N is negative. The plasma is assumed frozen on the timescale of the reflectometer probe beam (e.g. kHz perturbations compared to GHz probe beam frequency) and the calculation is made in a time-independent manner. The magnetic field remains finite across the resonance allowing a calculation of the electric field using Ampère’s law (a small, constant loss term is used to keep the to keep the electric field finite). A Gaussian modulated sinusoidal density perturbation is launched down the density gradient and the resulting perturbation to the reflectometer electric field is monitored in the vacuum region. The density perturbation is modelled to perturb the angle between the wave electric field and the local density gradient by assuming a finite density perturbation wavelength perpendicular to the density gradient ([35] uses a similar picture).

Results from this model are shown in figure 7 where the angle between the electric field and density gradient is varied locally by a small amount, ± 1 degree about a mean of 1 degree. Figure 7(a) shows the phase perturbation where the backscattering component is centred near $r = 79$ cm while the perturbation due to the resonance absorption is observed

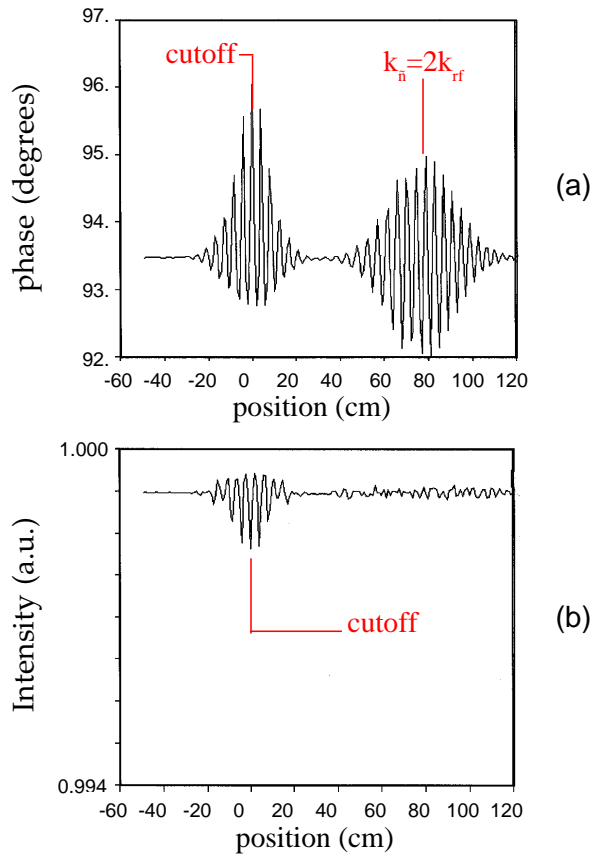


Figure 7. Results from 1D, full-wave simulation of resonance absorption effects on reflectometry. (a) Reflectometer phase signal, and (b) total returned reflectometer amplitude signal.

centred at the cut-off layer ($r = 0$). The position of the backscattered component is centred at the wavenumber matching condition $k_{\bar{n}} = 2k_0 N(r)$ in agreement with other 1D simulations. Figure 7(b) shows the amplitude variation for the same perturbation where only the absorption process produces a significant response. The total returned power is plotted and not the power at one point in the vacuum region. Since the scattering process conserves energy no signal is lost whereas the resonance process couples energy to the plasma resulting in a net loss. Both the phase and amplitude response are similar in shape to the density perturbation.

These results are consistent with the resonance absorption process occurring very near the cut-off and producing both an amplitude and a phase variation of the returned signal. Note that the spatial location of this effect is independent of the perturbation wavenumber. That is, the resonant absorption effect does not have a sensitivity cut-off at $k_{\bar{n}} = 2k_0$ as does the backscattered contribution. This effect may explain the results reported in [11] as it produces both an amplitude and phase variation centred at the cut-off region (independent of the perturbation wavenumber). Correlations between two homodyne reflectometer signals would benefit from the signals originating from the cut-off, thus providing a much lower possible radial correlation length than that from the phase alone. It is observed that the

backscattered component in figure 7(a) (at $r = 79$ cm) corresponds to the first term on the right-hand side of equation (3), $E_0 e^{i\tilde{\phi}}$, the pure phase term, while the response at the cut-off layer ($r = 0$) is due to the full expression, $(E_0 + \tilde{E}) e^{i\tilde{\phi}}$, which includes the amplitude variation. Thus, the inclusion of an intrinsic amplitude variation, that is, one arising from amplitude changes within the plasma, can result in a real amplitude variation of the reflectometer signal, localization of the perturbation to the cut-off, and a much broader wavenumber response.

This model is a 1D simulation of a problem which is, in general, 3D. It is not clear how this effect would translate to a 2 or 3D simulation. The size of the calculated phase perturbation is similar to that predicted for backscattering making it difficult to experimentally differentiate the two. X-mode polarization (using either the left- or right-hand cut-off) does not in general have a similar resonance near the cut-off. In that case, the upper hybrid resonance (while sometimes close) is often many wavelengths away from the right-hand cut-off making resonance absorption an unlikely general explanation for X-mode reflectometry. Nevertheless, it is important to note that this model does demonstrate that amplitude variations can induce a reflectometer response localized near the cut-off layer which does not follow the Bragg scattering rules. It is possible that a full 2 or 3D treatment of this effect might prove fruitful.

4. Summary and conclusions

In this paper the role of fluctuations in the reflectometer signal amplitude (as well as the phase) was investigated. Comparison of the homodyne reflectometer signal ($S_{\text{Re}} = E(t) \cos(\phi(t))$) and Langmuir probe data show broad agreement in power spectra and correlation lengths. These data indicate that the homodyne reflectometer signal can closely correspond to the density fluctuations. For low fluctuation levels the phase does agree with the homodyne signal; however, this agreement is lost at higher fluctuation levels where an unphysical (in terms of the density fluctuations) $1/f^2$ phase spectrum is observed. Thus at high fluctuation levels the homodyne signal is a good representation of the fluctuation behaviour while at low fluctuation levels either the homodyne or phase signal could be used. These observations are believed to be related to the fact that the reflectometer signal is linear in its response to \tilde{E} for all \tilde{E} but is linear in $\tilde{\phi}$ only at low fluctuation levels (equations (3) and (4), respectively). The data also indicate that the homodyne signal (composed of both an amplitude and phase component) is dominated by the amplitude at high fluctuation levels and that this is the portion of the signal that provides good agreement with Langmuir probes. The homodyne signal may, however, carry some important information on the sign of the fluctuation that is lost when the amplitude is calculated.

Consistency as well as areas of disagreement were found with some recent models. In particular, the phase predictions of [23] are consistent with the data here; however, the amplitude predictions are not consistent. RMS data and correlation lengths reported herein appear to be qualitatively consistent with the model of [33] although the comparison was necessarily limited. A 1D, full-wave model was presented in this paper which served as an illustration of the effect of amplitude fluctuations upon the reflectometer as well as how these fluctuations might arise from a simple model. That this simple model produced some of the observed behaviour (localization to cut-off, wavenumber response, both amplitude and phase fluctuations) is intriguing. However, this model is not believed to be general enough to explain the observations from many machines (where, for example, X-mode reflectometry is often used). Research remains to be done on the source of the amplitude

fluctuations, for example target size fluctuations, absorption, evanescent wave physics, etc. In addition, the distance and illuminated spot size dependences of the signal as well as exact dependence on reflectometer wavelength and various scale lengths (∇n_e , ∇B , or ∇N) remain to be investigated.

It is clear from the data reported here that the amplitude fluctuation as evidenced in the homodyne signal is an important component and should be incorporated into any complete reflectometer theory. This and the previous work of many others indicate that the reflectometer not only remains an important diagnostic tool for plasma science, but that it has the potential to provide even more detailed information on density fluctuation behaviour.

Acknowledgments

The excellent work of the CCT team and the DIII-D operations group is gratefully acknowledged. This work was supported by USDOE grant DE-FG03-86-ER53225, contract DE-AC03-89ER51114, and USDOE grant DE-FG03-89ER51121.

References

- [1] Costley A E, Cripwell P and Prentice R 1990 *Rev. Sci. Instrum.* **61** 2823
- [2] Doyle E J *et al* 1991 *Phys. Fluids B* **3** 2300
- [3] Estrada T *et al* 1990 *Rev. Sci. Instrum.* **61** 3034
- [4] Mazzucato E and Nazikian R 1991 *Plasma Phys. Control. Fusion* **33** 261
- [5] Hanson G R *et al* 1992 *Nucl. Fusion* **32** 1593
- [6] Senties J M *et al* 1989 *Controlled Fusion and Plasma Physics (Proc. 16th Eur. Conf., Venice, 1989)* vol 13B (European Physical Society) p 51
- [7] Doyle E J *et al* 1990 *Controlled Fusion and Plasma Physics (Proc. 17th Eur. Conf. Amsterdam, 1990)* vol 14B (European Physical Society) p 203
- [8] Paulett C Liewer 1985 *Nucl. Fusion* **25** 543
- [9] Baang S *et al* 1990 *Rev. Sci. Instrum.* **61** 3013
- [10] Cripwell P and Costley A E 1991 *Proc. 18th Eur. Conf. (Berlin, 1991)* vol 15C (European Physical Society) p I-17
- [11] Rhodes T L *et al* 1992 *Rev. Sci. Instrum.* **63** 4599
- [12] Rhodes T L *et al* 1995 *Rev. Sci. Instrum.* **66** 824
- [13] Xu Hong-Liang, Cao Jin-Xiang, Ding Wei-Xing, Yu Chang-Xuan 1996 *Chin. Phys. Lett.* **13** 374
- [14] Ginzburg V L 1960 *Propagation of Electromagnetic Waves in Plasmas* (New York: Gordon and Breach)
- [15] Pitteway M L 1958 *Proc. R. Soc. A* **252** 556
- [16] Hutchinson I H 1992 *Plasma Phys. Control. Fusion* **34** 1225
- [17] Bretz N 1992 *Phys. Fluids B* **4** 2414
- [18] Irby J H, Horne S, Hutchinson I H and Stek P C 1993 *Plasma Phys. Control. Fusion* **35** 601
- [19] Fanack C *et al* 1996 *Plasma Phys. Control. Fusion* **38** 1915
- [20] Albert E Chou, Afeyan B B and Cohen B I 1995 *Rev. Sci. Instrum.* **66** 1216
- [21] Holzhauser E and Rhodes T L 1992 *Proc. IAEA Technical Committee Meeting on Reflectometry at the JET Joint Undertaking (4-6 March, 1992)* p 97
- [22] Taylor R J *et al* 1989 *Phys. Rev. Lett.* **63** 2365
- [23] Mazzucato E and Nazikian R 1993 *Phys. Rev. Lett.* **71** 1840
- Nazikian R and Mazzucato E 1995 *Rev. Sci. Instrum.* **66** 392
- [24] Luxon J, The DIII-D Team 1995 *Fusion Engineering and Design* vol 30 (Elsevier) pp 39-52
- [25] Rhodes T L *et al* 1993 *Nucl. Fusion* **33** 1787
- [26] Ritz Ch P *et al* 1984 *Phys. Fluids* **27** 2956
- [27] Ritz Ch P 1991 *Plasma Physics and Controlled Nuclear Fusion Research 1990 (Proc. 13th Int. Conf. Washington, DC 1990)* vol 2 (Vienna: IAEA) p 589
- [28] Krämer M and Carlson A 1989 *Controlled Fusion and Plasma Physics (Proc. 16th Eur. Conf., Venice, 1989)* vol 13B (European Physical Society) p 923
- [29] Zweben S J and Gould R W 1985 *Nucl. Fusion* **25** 171
- [30] Bruskin L G, Mase A and Tamano T 1996 *J. Plasma Fusion Res.* **72** 356-64

- [31] Massey G A 1984 *Appl. Opt.* **23** 658
- [32] Moyer R A *et al* 1995 *Phys. Plasmas* **2** 2397
- [33] Conway G D, Schott L and Hirose A 1996 *Plasma Phys. Control. Fusion* **38** 451
- [34] White R B and Chen F F 1974 *Plasma Phys.* **16** 565
- [35] Stenzel R L *et al* 1974 *Phys. Rev. Lett.* **32** 654
- [36] Thomson J J *et al* 1976 *Phys. Rev. Lett.* **37** 1052